Imaging of Infection and Inflammation with an Improved ^{99m}Tc-Labeled LTB4 Antagonist

Julliëtte E.M. van Eerd, MSc[1]; Matthias Broekema, MSc[2]; Thomas D. Harris, PhD[3]; D. Scott Edwards, PhD[3]; Wim J.G. Oyen, MD[1]; Frans H.M. Corstens, MD[1]; and Otto C. Boerman, PhD[1]

[1]Department of Nuclear Medicine, Radboud University Nijmegen Medical Centre, Nijmegen, The Netherlands;
[2]Department of Medicinal Chemistry, Utrecht University, Utrecht, The Netherlands; and [3]Discovery Research, Bristol-Myers Squibb Medical Imaging, North Billerica, Massachusetts

Studies have demonstrated that the bivalent ^{111}In-labeled leukotriene B4 (LTB4) antagonist DPC11870 reveals infectious and inflammatory lesions in various rabbit models. The radioactive tracer accumulates quickly at the site of infection and clears rapidly from the circulation, resulting in high-quality images. In this study, 2 new hydrazinonicotinamide (HYNIC)-conjugated compounds that are structurally related to DPC11870 were studied to further improve image quality. **Methods:** A bivalent HYNIC-conjugated LTB4 antagonist (MB81) and a monovalent one (MB88) were labeled with ^{99m}Tc. The radiolabeled compounds were intravenously injected into New Zealand White rabbits with *E. coli* infection in the left thigh muscle. The imaging characteristics of both compounds were compared with those of the bivalent ^{111}In-labeled LTB4 antagonist. **Results:** Both ^{99m}Tc-labeled LTB4 antagonists revealed the abscess from 2 h after injection onward. Abscess uptake at 8 h after injection was similar for both compounds (0.22 ± 0.08 percentage injected dose per gram [%ID/g] and 0.36 ± 0.13 %ID/g for the bivalent and monovalent compounds, respectively). However, visualization of the abscess and the quality of the images were better after injection of MB88 than after injection of either of the bivalent LTB4 antagonists. The excellent delineation of the abscess by MB88 was mainly due to the more rapid clearance of this compound from nontarget organs. **Conclusion:** The ^{99m}Tc-labeled HYNIC conjugated LTB4 antagonists MB88 and MB81 revealed infectious foci in rabbits within a few hours after injection. Imaging characteristics of monovalent ^{99m}Tc-MB88 were superior to those of the bivalent LTB4 antagonists DPC11870 and MB81. Therefore, of the 3 LTB4 antagonists, the monovalent LTB4 antagonist MB88 is the most potent and promising agent for visualizing and evaluating infection and inflammation in patients.

Key Words: LTB4 antagonist; infection imaging; scintigraphy

J Nucl Med 2005; 46:1546–1551

Detection and localization of infectious and inflammatory lesions is important for appropriate treatment. One method of detecting infection and inflammation is scintigraphy. For scintigraphic detection of inflammatory and infectious lesions in patients, ^{67}Ga-citrate and radiolabeled leukocytes are the most commonly applied radiopharmaceuticals (*1*). However, there is a continuous search for new radiopharmaceuticals that allow rapid and accurate visualization of the lesions and that lack the disadvantages of currently used compounds (e.g., laborious and time-consuming preparation and contamination risks) (*2*). Chemotactic and chemokinetic peptides and their antagonists are attractive candidates for this application (*3*). These compounds accumulate at the site of infection because of specific receptor interaction and clear rapidly from nontarget tissues. Compounds such as interleukin-2, interleukin-8, and platelet factor 4 accumulate at the site of infection because of specific interaction with receptors expressed on activated and infiltrated granulocytes (*4–6*). The leukotriene B4 (LTB4) receptor, expressed on polymorphonuclear granulocytes, is involved in leukocyte function during the inflammatory response (*7,8*). Several studies have been performed with a radiolabeled LTB4 antagonist to visualize infection and inflammation by targeting its specific receptors expressed on activated and infiltrated neutrophils (*9,10*). The LTB4 antagonist ^{111}In-DPC11870 rapidly revealed infectious and inflammatory lesions in several rabbit models of acute inflammation (*11,12*). The compound cleared rapidly from the nontarget tissues, and physiologic uptake was seen only in the spleen, bone marrow, and kidneys. In an in vivo receptor-blocking experiment, we demonstrated that accumulation at the site of infection was receptor mediated (*10*).

Although the promising characteristics of ^{111}In-DPC11870 warranted clinical evaluation in patients, for this application a ^{99m}Tc-labeled tracer is preferred. The use of ^{99m}Tc could improve image resolution and would reduce the radiation dose to the patient. Therefore, 2 analogs of DPC11870 were synthesized in which the diethylenetriaminepentaacetic acid (DTPA) chelator was replaced by the bifunctional chelator succinimidyl-hydrazinonicotinamide (S-HYNIC). One compound was structurally almost identical to DPC11870, differing only in metal ligand, and consisted of 2 LTB4 receptor-binding sites. The other LTB4 antagonist was a

monomeric derivative of DPC11870 consisting of 1 LTB4 binding site and again conjugated with HYNIC. In this study, we labeled both LTB4 antagonists with ^{99m}Tc and compared the imaging characteristics of both compounds with those of ^{111}In-DPC11870.

MATERIALS AND METHODS

Radiolabeling

The chemical structures of the 2 HYNIC-conjugated LTB4 antagonists are presented in Figure 1. Synthesis of the HYNIC-conjugated LTB4 antagonist MB81 (bivalent, BMS57868-81) and MB88 (monovalent, BMS57868-88) will be described in detail elsewhere. MB81 and MB88 (25 μg) were labeled with 555 MBq of Na-^{99m}TcO$_4$ (Tyco Healthcare Mallinckrodt) in the presence of 15 mg of tricine and 2 mg of isonicotinic acid in 350 μL of phosphate-buffered saline, pH 7.0, and 25 μL of SnSO$_4$ (1 mg/mL) in 0.1N HCl. After incubation for 30 min at 100°C, quality control was performed using reverse-phase high-performance liquid chromatography (HPLC) (1100 series; Agilent Technologies) on a C18 column (Zorbax Rx-C18, 4.6 × 250 mm; Agilent Technologies) at a flow rate of 1 mL/min with a gradient mobile phase from 100% ammonium acetate (10 mmol/L; pH 7.2) to 100% acetonitrile in 20 min.

DPC11870 was labeled with ^{111}InCl$_3$ (Tyco Healthcare Mallinckrodt) as described previously (10,12). The 20 μg of LTB4 antagonist DPC11870 were labeled with 74 MBq of ^{111}In. Quality control of the DPC11870 compound was performed using the same HPLC protocols as described above.

Infection Model

Fifteen female New Zealand White rabbits weighing 2.3–2.8 kg were kept in cages (1 rabbit per cage) and fed standard laboratory chow and water ad libitum. The rabbits were anesthetized by subcutaneous injection of 0.7 mL of a mixture of fentanyl (0.315 mg/mL) and fluanisone (10 mg/mL) (Hypnorm; Janssen Pharmaceutica). Twenty minutes afterward, an *E. coli* infection was induced in the left thigh muscle by intramuscular injection of 4 × 10^9 colony-forming units of *E. coli* bacteria.

All animal experiments were approved by the local animal welfare committee in accordance with the guidelines of the Dutch legislation.

Imaging and Biodistribution

Twenty-four hours after induction of the abscess, when swelling of the infected muscle was apparent, tracer was injected via the lateral ear vein. Five rabbits received 37 MBq of ^{99m}Tc-MB81 (3.0 μg), 5 received 37 MBq of ^{99m}Tc-MB88 (3.0 μg), and 5 received 11 MBq of ^{111}In-DPC11870 (3.0 μg). For scintigraphic imaging, the rabbits were immobilized in a mold and placed prone on a γ-camera (Orbiter; Siemens), using a low-energy parallel-hole collimator for the ^{99m}Tc-labeled compounds and a medium-energy collimator for the ^{111}In-labeled compound. Images (300,000 counts per image) were obtained at several times, starting immediately after injection and continuing until 8 h after injection, and were stored digitally in a 256 × 256 matrix. All images were adjusted to the same background and intensity levels, allowing a fair comparison among them. The scintigraphic results were analyzed using regions of interest drawn over the heart, lungs, liver, spleen, kidneys, bone marrow, abscess, and contralateral muscle (background). Abscess-to-organ ratios were calculated. Blood samples were drawn at 1, 3, 5, 10, 30, 60, 120, 240, and 480 min after injection. The activity in the samples was determined in a γ-counter (Wizard; Canberra Packard) and expressed as a percentage of the injected dose (%ID), assuming that the total blood weight accounted for 6% of the total body weight (13). The distribution half-life (t$_{1/2}$α) and clearance half-life (t$_{1/2}$β) were calculated assuming a 2-phase linear model for blood clearance. At 8 h after injection, all rabbits were euthanized. A blood sample was taken by cardiac puncture. Tissues were dissected and weighed. The activity in tissues was measured in a shielded well-type γ-counter together with the injection standards and was expressed as %ID/g.

Statistical Analysis

All mean values are presented as mean ± SD. Statistical analysis was performed using 1-way ANOVA. Results were corrected for multiple datasets with the Bonferroni multiple-comparisons test. The level of significance was set at 0.05.

RESULTS

Radiolabeling

Results of the HPLC radioactivity analysis indicated that both the bivalent MB81 and the monovalent MB88 could be labeled with ^{99m}Tc with a specific activity of 37 MBq/μg (110 MBq of MB81 and 60 MBq of MB88 per nanomole). The labeling efficiency exceeded 95%. Reverse-phase
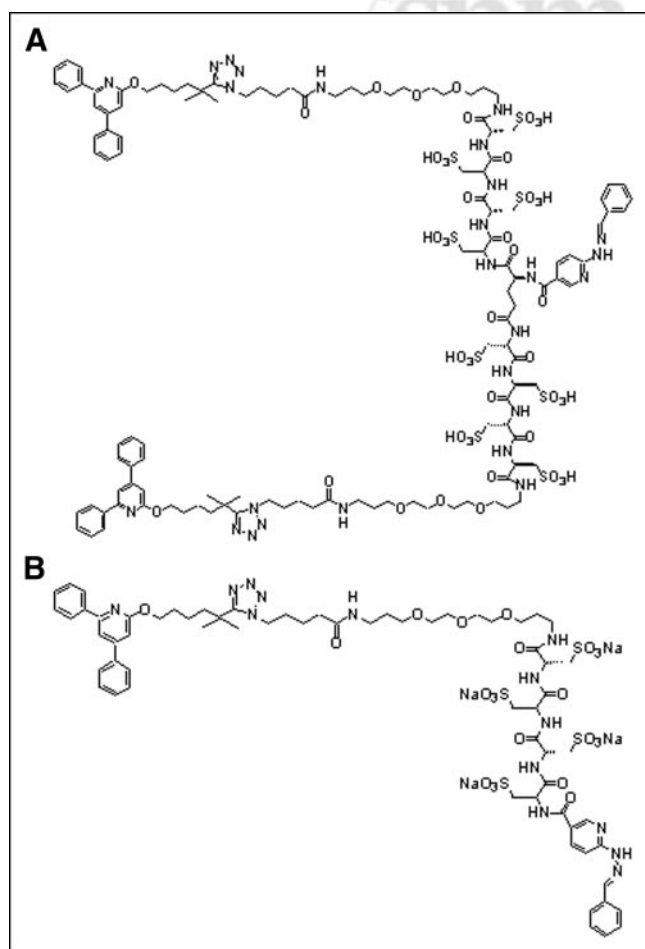
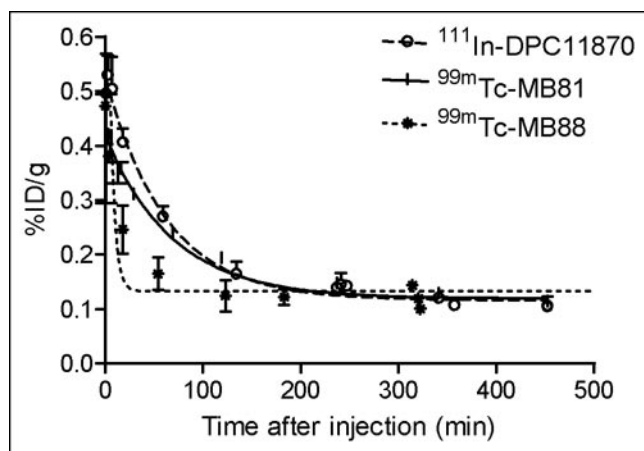**FIGURE 1.** Chemical structures of MB81 (A) and MB88 (B).

HPLC analysis showed that the labeling efficiency of DPC11870 was more than 95%, with a specific activity of 3.7 MBq/μg (12 MBq/nmol).

Imaging and Biodistribution

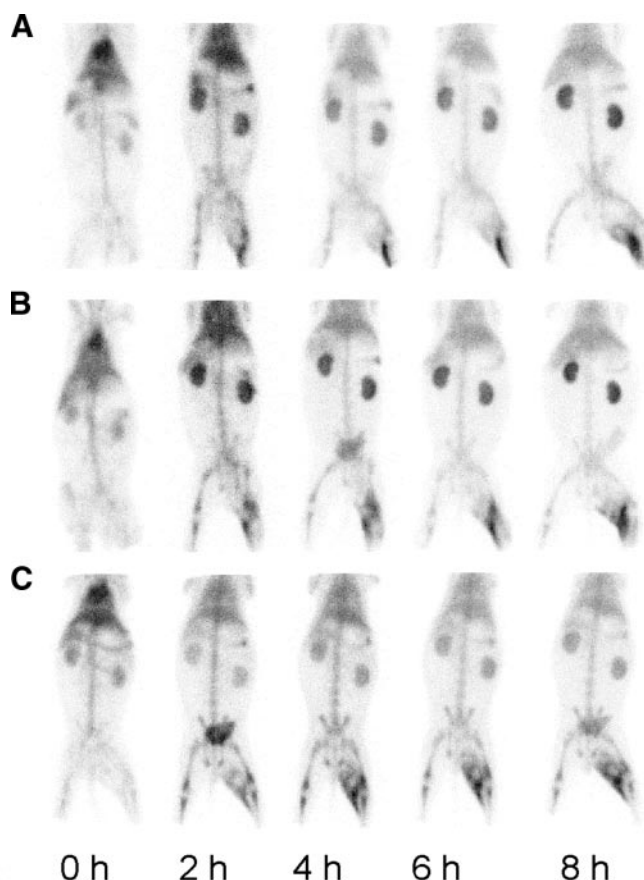Analysis of the blood samples indicated that ^{99m}Tc-MB88 cleared rapidly from the circulation (Fig. 2). The $t_{1/2}\alpha$ was 7 min for ^{99m}Tc-MB88 and 20 min for the bivalent ^{99m}Tc-labeled antagonist MB81. $t_{1/2}\beta$ also differed between the ^{99m}Tc-labeled LTB4 antagonists. The $t_{1/2}\beta$ of the monovalent MB81 was 16.5 h, whereas the $t_{1/2}\beta$ of ^{99m}Tc-MB88 was much longer (85.6 h).

Scintigraphic images after injection of the bivalent ^{111}In-DPC11870, the bivalent ^{99m}Tc-MB81, and the monovalent ^{99m}Tc-MB88 are shown in Figure 3. Immediately after injection, the whole-body distribution of all 3 radiolabeled LTB4 antagonists was similar. Accumulation of radioactivity was observed in the lungs, liver, kidneys, and bone marrow of all animals. At 2 h after injection of the 3 LTB4 antagonists, the abscesses could already be visualized in all animals. However, images acquired with the monovalent LTB4 antagonist at that time were qualitatively superior to images acquired with either bivalent antagonist. Images acquired at 2 h or later indicated that the monovalent MB88 cleared more rapidly from the circulation and nontarget tissues than did the bivalent LTB4 antagonists MB81 and DPC11870. Additionally, compared with the other 2 LTB4 compounds, MB88 showed a low radioactivity concentration in the kidneys. Because of the low radioactivity concentration in nontarget tissues, visualization of the abscess was better in animals injected with ^{99m}Tc-MB88 than in animals injected with either ^{111}In-DPC11870 or ^{99m}Tc-MB81 at the same time point.

Abscess-to-organ ratios calculated from region-of-interest analysis of images acquired 8 h after injection are shown


FIGURE 3. Anterior images of rabbits in which intramuscular infection was induced. Images were acquired immediately and 2, 4, 6, and 8 h after injection of 11 MBq of ^{111}In-DPC11870 (A), 37 MBq of ^{99m}Tc-MB81 (B), or 37 MBq of ^{99m}Tc-MB88 (C).

FIGURE 2. Blood clearance of ^{111}In-DPC11870, ^{99m}Tc-MB81, and ^{99m}Tc-MB88 in New Zealand White rabbits. Average amount of radioactivity of 3 rabbits is expressed as %ID/g present in blood. Curves represent best nonlinear exponential decay calculated by Prism software program (GraphPad Software, Inc.).

in Figure 4. When the HYNIC-conjugated antagonists were compared, only a few differences between the monovalent and the bivalent compounds were observed. The abscess-to-kidney ratio was significantly higher for the monovalent ^{99m}Tc-MB88 than for the bivalent ^{99m}Tc-MB81 ($P < 0.0001$). Furthermore, of all the organs and tissues, the abscess had the highest radioactivity concentration of MB88, because all ratios of the monovalent LTB4 antagonist exceeded 1. When ratios of MB88 were compared with those of ^{111}In-DPC11870, only the abscess-to-kidney ratio differed significantly ($P < 0.01$). The abscess-to-organ ratios of the 2 bivalent radiolabeled compounds (^{99m}Tc-MB81 and ^{111}In-DPC11870) were similar.

The biodistribution data derived from ex vivo counting of dissected tissues, as summarized in Figure 5, agreed with the scintigraphic images. Blood levels of both ^{99m}Tc-labeled compounds were low (0.10 ± 0.01 %ID/g and 0.09 ± 0.01 %ID/g for, respectively, the bivalent and the monovalent ^{99m}Tc-labeled compounds at 8 h after injection). Furthermore, abscess uptake did not differ significantly between the 2 HYNIC-conjugated antagonists (0.22 ± 0.08 %ID/g and 0.36 ± 0.13 %ID/g). However, the radioactivity concentration significantly differed between compounds in the liver
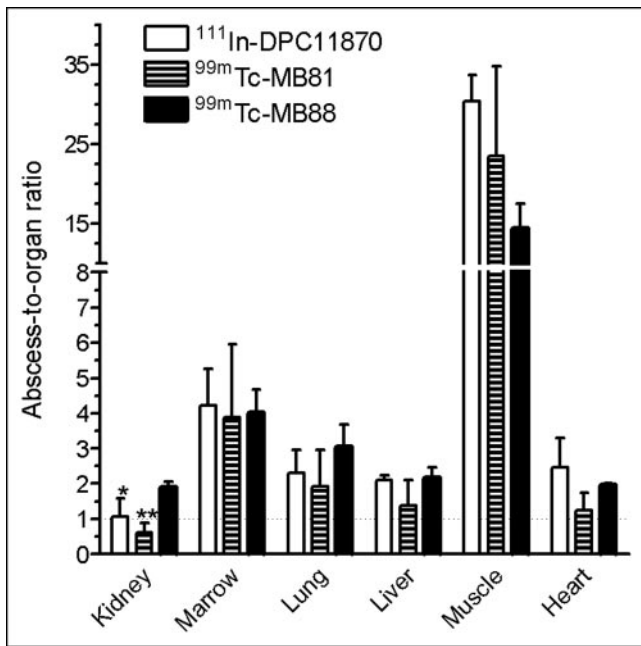
FIGURE 4. Abscess-to-organ ratios calculated from region-of-interest data obtained from images acquired 8 h after injection of ¹¹¹In-DPC11870, ⁹⁹ᵐTc-MB81, or ⁹⁹ᵐTc-MB88. *$P < 0.05$. **$P < 0.01$.

and compounds in the kidneys. Kidney uptake of ⁹⁹ᵐTc-MB88 was significantly lower than that of the bivalent ⁹⁹ᵐTc-MB81 (0.58 ± 0.06 %ID/g) ($P < 0.001$). Also, the radioactivity concentration in the liver was higher after injection of ⁹⁹ᵐTc-MB81. When the results for the HYNIC-conjugated antagonists were compared with those for the initially synthesized reference compound (¹¹¹In-DPC11870), more differences were found. First, the radioactivity concentration in the bone marrow was much higher with ¹¹¹In-DPC11870 (0.57 ± 0.19 %ID/g) than with either of the ⁹⁹ᵐTc-labeled compounds (0.26 ± 0.1 %ID/g and 0.25 ± 0.06 %ID/g for MB81 and MB88, respectively). Second, kidney uptake of ¹¹¹In-DPC11870 was low and

significantly different from that of the bivalent ⁹⁹ᵐTc-MB81 ($P < 0.001$). However, kidney uptake of ¹¹¹In-DPC11870 was comparable with that of the monovalent ⁹⁹ᵐTc-MB88. Third, significant differences were found among the radioactivity concentrations of the 3 compounds in liver and spleen. In both organs, the concentration of ⁹⁹ᵐTc-MB88 was lowest (0.07 ± 0.01 %ID/g and 0.25 ± 0.01 %ID/g for liver and spleen, respectively). Spleen and bone marrow were the organs that contained the highest radioactivity concentrations of ¹¹¹In-DPC11870. For the bivalent ⁹⁹ᵐTc-MB81, the highest concentration was found in the kidneys, whereas for the monovalent ⁹⁹ᵐTc-MB88, the highest concentration was found in the abscess. As a result, the abscess was best visualized with ⁹⁹ᵐTc-MB88.

DISCUSSION

In previous studies, we demonstrated that the bivalent ¹¹¹In-labeled LTB4 antagonist DPC11870 adequately revealed infectious and inflammatory foci in distinct rabbit models (10–12). Although the results of previous studies warranted clinical studies, we synthesized 2 HYNIC-conjugated analogs of this compound to allow radiolabeling with ⁹⁹ᵐTc. In this study, the imaging characteristics of ¹¹¹In-DPC11870 were compared with those of the ⁹⁹ᵐTc-labeled bivalent analog MB81 and the ⁹⁹ᵐTc-labeled monovalent derivative MB88.

The results of the imaging and biodistribution experiments indicated that, besides ¹¹¹In-DPC11870, both ⁹⁹ᵐTc-labeled antagonists revealed infectious foci within a few hours after injection. Furthermore, both MB81 and MB88 showed physiologic uptake in bone marrow, spleen, and, kidneys. The radioactivity concentration of the infected tissue at 8 h after injection was similar for both ⁹⁹ᵐTc-labeled compounds. The radioactivity concentration of the monovalent ⁹⁹ᵐTc-MB88 in the kidneys was much lower than that of the bivalent ⁹⁹ᵐTc-MB81. Comparison of the ⁹⁹ᵐTc-labeled bivalent and monovalent LTB4 antagonists revealed that images acquired after injection of the mono-
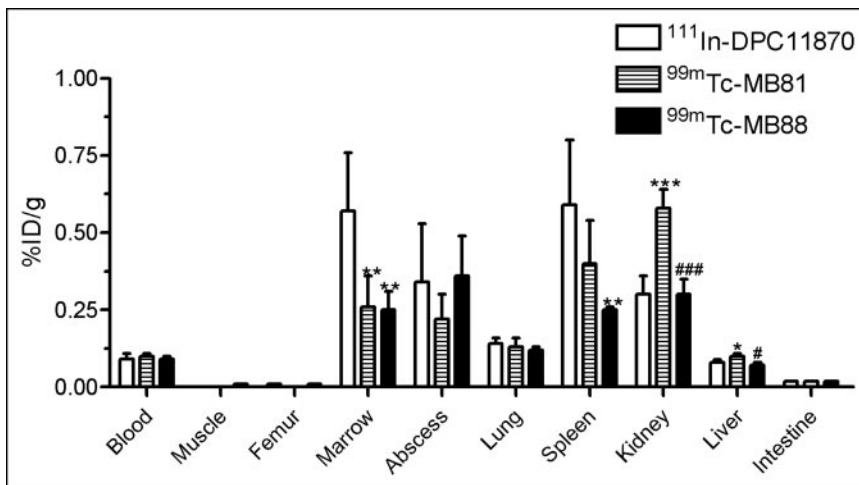
FIGURE 5. Biodistribution data obtained 8 h after injection of ¹¹¹In-DPC11870, ⁹⁹ᵐTc-MB81, or ⁹⁹ᵐTc-MB88. Each bar represents mean value $\pm$ SD. Values were analyzed using ANOVA. *$P < 0.05$, **$P < 0.01$, and ***$P < 0.001$ for ¹¹¹In-DPC11870 vs. ⁹⁹ᵐTc-MB81 or ⁹⁹ᵐTc-MB88. #$P < 0.05$, ##$P < 0.01$, and ###$P < 0.001$ for ⁹⁹ᵐTc-MB81 vs. ⁹⁹ᵐTc-MB88.

valent ^{99m}Tc-MB88 allowed superior abscess visualization because of fast clearance of ^{99m}Tc-MB88 from nontarget tissues and good accumulation of radioactivity in the abscess. Additionally, the abscess was delineated earlier with ^{99m}Tc-MB88 than with the bivalent analog. Delineation of the abscess was worse with the bivalent ^{99m}Tc-MB81 than with ^{99m}Tc-MB88 because images were scaled identically, based on the pixels with the highest radioactivity concentration. Because of the high kidney uptake after injection of ^{99m}Tc-MB81, the amount of radioactivity in the abscess seemed to be lower but was equal, as determined in the biodistribution experiment. When the characteristics of the best-performing ^{99m}Tc-labeled antagonist, MB88, were compared with those of ^{111}In-DPC11870, the images acquired after injection of the ^{99m}Tc-compound were again superior. In this case, despite similar abscess and kidney uptake, better images were obtained because of lower radioactivity concentrations in the bone marrow of animals injected with the monovalent ^{99m}Tc-MB88.

In a previous study, we cautiously analyzed the pharmacodynamics of the ^{111}In-labeled LTB4 antagonist DPC11870 (*14*). From the results of that study, we concluded that accumulation at the site of infection was based on initial targeting of receptor-positive cells in the bone marrow, followed by migration of radioactivity from the bone marrow to the site of infection. In addition we determined that, similarly to radiolabeled leukocytes, ^{111}In-DPC11870 showed physiologic uptake in spleen, liver, and bone marrow (*15,16*). The radioactivity concentration in the bone marrow after injection of both newly synthesized HYNIC-conjugated LTB4 antagonists was lower than that after injection of ^{111}In-DPC11870. The lower bone marrow concentration was an important factor determining the quality of abscess visualization after injection of the ^{99m}Tc-labeled compounds. The rapid blood clearance of the monomeric LTB4 antagonist may explain the low bone marrow uptake. However, because blood clearance was similar for both bivalent compounds (^{99m}Tc-labeled and ^{111}In-labeled), a difference in blood clearance could not explain the lower bone marrow uptake of the bivalent ^{99m}Tc-MB81. Another explanation for the lower bone marrow uptake of both HYNIC compounds might be the introduction of the HYNIC chelator, which could affect the kinetics of the compound. The low radioactivity concentration of both HYNIC compounds in the spleen supports this explanation.

The present results indicate that the chelator (HYNIC or DTPA) obviously affected the in vivo behavior and biodistribution of the radiolabeled LTB4 antagonist. Several studies have focused on the in vivo effect of a chelator (*17,18*). These studies demonstrated that a chelator might affect the in vivo characteristics of a compound. In a comparative study in which the biodistribution of ^{99m}Tc-labeled and ^{111}In-labeled octreotide was evaluated, kidney retention of the ^{99m}Tc-labeled compound was found to be less than that of the ^{111}In-labeled compound (*19*). The characteristics of MB81 were less favorable than those of MB88 because of

the higher kidney retention and slower $t_{1/2}\alpha$ of the compound. Because the $t_{1/2}\alpha$ of ^{111}In-DPC11870 (30 min) is comparable with that of MB81, the longer $t_{1/2}\alpha$ of MB81 probably is caused by its bivalency. The higher radioactivity concentration of ^{99m}Tc-MB81 in the kidney is difficult to explain. Because kidney retention of both ^{111}In-DPC11870 (bivalent, DTPA) and ^{99m}Tc-MB88 (monovalent, HYNIC) was lower than that of ^{99m}Tc-MB81, it is not clear whether the kidney retention was caused by the bivalency or the HYNIC conjugation of the LTB4 antagonist. The high-quality images obtained with ^{99m}Tc-MB88 resulted from use of the high-resolution radiolabel ^{99m}Tc, rapid clearance of MB88 from nontarget tissue, and preserved accumulation of this LTB4 antagonist at the site of infection.

The ideal imaging agent for detection of infectious and inflammatory foci needs to satisfy several requirements. First, the agent should accumulate specifically and rapidly in the foci and clear quickly from the nontarget tissues to allow visualization of the lesion shortly after injection. Second, the labeling procedure should be relatively simple, and labeling should preferably be with ^{99m}Tc instead of other radionuclides. Finally, the agent should not provoke side effects when administered to patients (*20*). The results of the present study indicate that ^{99m}Tc-MB88 meets the requirements for a potential infection-imaging agent. When these results are compared with those for other currently studied compounds, ^{99m}Tc-MB88 remains a promising candidate. Other agents currently under investigation include other radiolabeled cytokines and chemotactic peptides (interleukin-2, interleukin-8, and platelet factor 4) (*4,21,22*). These compounds, however, exhibit biologic activity and have the disadvantage of provoking side effects in patients. Furthermore, production of these recombinant peptides is complicated and expensive. Antimicrobial agents (^{99m}Tc-ciprofloxacin [Infecton; Draximage Inc.] and human neutrophil peptides) (*23,24*) have an advantage over ^{99m}Tc-MB88 in that they may be targeted specifically at bacteria. Therefore, these agents can potentially differentiate between infectious lesions and inflammatory foci. Infecton has been evaluated in several clinical studies and yields a high overall sensitivity and specificity (85.4% and 81.7%, respectively) (*23*). Another advantage of Infecton over MB88 is lack of bone marrow uptake, possibly suiting Infecton for detection of infection after orthopedic interventions (e.g., osteomyelitis).

In summary, clinical evaluation of ^{99m}Tc-MB88 is warranted to assess its value as an infection-imaging agent and to allow a fair comparison with the other currently studied agents.

CONCLUSION

In the present study, we compared the imaging characteristics of 3 radiolabeled LTB4 antagonists for visualizing infection and inflammation. Visualization of infectious foci on images obtained with the monovalent LTB4 antagonist

^{99m}Tc-MB88 was superior to that on images obtained with the other 2 compounds. We consider ^{99m}Tc-MB88 to be a potent and promising agent for visualizing infection and inflammation in patients.

ACKNOWLEDGMENT

REFERENCES

1. Knight LC. Non-oncologic applications of radiolabeled peptides in nuclear medicine. *Q J Nucl Med.* 2003;47:279–291.
2. Weiner RE, Thakur ML. Radiolabeled peptides in diagnosis and therapy. *Semin Nucl Med.* 2001;31:296–311.
3. Signore A, Chianelli M, Bei R, Oyen WJ, Modesti A. Targeting cytokine/chemokine receptors: a challenge for molecular nuclear medicine. *Eur J Nucl Med Mol Imaging.* 2003;30:149–156.
4. Bleeker-Rovers CP, Boerman OC, Rennen HJ, Corstens FH, Oyen WJ. Radiolabeled compounds in diagnosis of infectious and inflammatory disease. *Curr Pharm Des.* 2004;10:2935–2950.
5. van Eerd JE, Boerman OC, Corstens FH, Oyen WJ. Radiolabeled chemotactic cytokines: new agents for scintigraphic imaging of infection and inflammation. *Q J Nucl Med.* 2003;47:246–255.
6. Signore A, Annovazzi A, Barone R, et al. ^{99m}Tc-Interleukin-2 scintigraphy as a potential tool for evaluating tumor-infiltrating lymphocytes in melanoma lesions: a validation study. *J Nucl Med.* 2004;45:1647–1652.
7. Pettersson A, Richter J, Owman C. Flow cytometric mapping of the leukotriene B4 receptor, BLT1, in human bone marrow and peripheral blood using specific monoclonal antibodies. *Int Immunopharmacol.* 2003;3:1467–1475.
8. Yokomizo T, Izumi T, Chang K, Takuwa Y, Shimizu T. A G-protein-coupled receptor for leukotriene B4 that mediates chemotaxis. *Nature.* 1997;387:620–624.
9. Brouwers AH, Laverman P, Boerman OC, et al. A ^{99m}Tc-labeled leukotriene B4 receptor antagonist for scintigraphic detection of infection in rabbits. *Nucl Med Commun.* 2000;21:1043–1050.
10. van Eerd JE, Oyen WJ, Harris TD, et al. A bivalent leukotriene B(4) antagonist for scintigraphic imaging of infectious foci. *J Nucl Med.* 2003;44:1087–1091.
11. van Eerd JE, Laverman P, Oyen WJ, et al. Imaging of experimental colitis with a radiolabeled leukotriene B4 antagonist. *J Nucl Med.* 2004;45:89–93.
12. van Eerd JE, Rennen HJ, Oyen WJ, et al. Scintigraphic detection of pulmonary aspergillosis in rabbits with a radiolabeled leukotriene b4 antagonist. *J Nucl Med.* 2004;45:1747–1753.
13. Jain NC, ed. *Shalm's Veterinary Hematology.* Vol 91. Philadelphia, PA: Lea and Febiger; 1986:87–102.
14. van Eerd JE, Oyen WJ, Harris TD, et al. Scintigraphic imaging of infectious foci with an ^{111}In-LTB4 antagonist is based on in-vivo labeling of granulocytes. *J Nucl Med.* 2005;46:786–793.
15. Hughes DK. Nuclear medicine and infection detection: the relative effectiveness of imaging with ^{111}In-oxine-, ^{99m}Tc-HMPAO-, and ^{99m}Tc-stannous fluoride colloid-labeled leukocytes and with ^{67}Ga-citrate. *J Nucl Med Technol.* 2003;31:196–201.
16. Love C, Palestro CJ. Radionuclide imaging of infection. *J Nucl Med Technol.* 2004;32:47–57.
17. Ono M, Arano Y, Mukai T, et al. Plasma protein binding of (99m)Tc-labeled hydrazino nicotinamide derivatized polypeptides and peptides. *Nucl Med Biol.* 2001;28:155–164.
18. Qu T, Wang Y, Zhu Z, Rusckowski M, Hnatowich DJ. Different chelators and different peptides together influence the in vitro and mouse in vivo properties of ^{99m}Tc. *Nucl Med Commun.* 2001;22:203–215.
19. Decristoforo C, Melendez-Alafort L, Sosabowski JK, Mather SJ. ^{99m}Tc-HYNIC-[Tyr3]-octreotide for imaging somatostatin-receptor-positive tumors: preclinical evaluation and comparison with ^{111}In-octreotide. *J Nucl Med.* 2000;41:1114–1119.
20. Corstens FH, van der Meer JW. Chemotactic peptides: new locomotion for imaging of infection? *J Nucl Med.* 1991;32:491–494.
21. Rennen HJ, Boerman OC, Oyen WJ, Corstens FH. Kinetics of ^{99m}Tc-labeled interleukin-8 in experimental inflammation and infection. *J Nucl Med.* 2003;44:1502–1509.
22. Signore A, Procaccini E, Annovazzi A, Chianelli M, van der Laken C, Mire-Sluis A. The developing role of cytokines for imaging inflammation and infection. *Cytokine.* 2000;12:1445–1454.
23. Britton KE, Wareham DW, Das SS, et al. Imaging bacterial infection with ^{99m}Tc-ciprofloxacin (Infecton). *J Clin Pathol.* 2002;55:817–823.
24. Welling MM, Nibbering PH, Paulusma-Annema A, Hiemstra PS, Pauwels EK, Calame W. Imaging of bacterial infections with ^{99m}Tc-labeled human neutrophil peptide-1. *J Nucl Med.* 1999;40:2073–2080.